Spring 5-12-2018

FLAME RETARDANCY OF FERROCENE INCORPORATED EPOXIDE

Sultan Alanazi
Pittsburg State University, sultan.alanazi@gus.pittstate.edu

FLAME RETARDANCY OF FERROCENE INCORPORATED EPOXIDE

A Thesis Submitted to the Graduate School
in Partial Fulfillment of the Requirements
for the Degree of
Master of Science

Sultan Alanazi

Pittsburg State University

Pittsburg, Kansas

May, 2018

FLAME RETARDANCY OF FERROCENE
INCORPORATED EPOXIDE

Sultan Alanazi

APPROVED:

Thesis Advisor _____
Dr. Jody Neef, Department of Chemistry

Committee Member _____
Dr. Khamis Siam, Department of Chemistry

Committee Member _____
Dr. Santimukul Santra, Department of Chemistry

Committee Member _____
Dr. Benjamin Tayo, Department of Physics

ACKNOWLEDGEMENTS

First and foremost, I would like to thank God Almighty for giving me the strength, knowledge and ability to finish my thesis. In my journey towards this degree, I have found a teacher, a friend, and inspiration to me in the research. I would like to say thanks to Dr. Neef, for his advice and guidance for helping me to write my thesis step by step. I would like to thank the rest of my thesis committee members: Dr. Khamis Siam, Dr. Santimukul Santra and Dr. Benjamin Tayo.

I also thank my family who encouraged me and prayed for me throughout the time of my research. Also, I am thankful to my friends who helped and encouraged me in difficult time of my life to graduate.

FLAME RETARDANCY OF FERROCENE
INCORPORATED EPOXIDE

An Abstract of the Thesis by
Sultan Alanazi

Epoxy resins are thermosetting resins that are used in a variety of applications such as electrical and electronic devices. However, epoxy resins can be inherently flammable. To circumvent this problem, epoxy resins were prepared by incorporating ferrocene carboxylic acid into the epoxy prior to thermal setting, as a flame retardant. Ferrocene carboxylic acid was prepared by condensing o-chlorobenzoyl chloride with ferrocene followed by hydrolysis. The synthesized ferrocene carboxylic acid was characterized by ^{1}H-NMR spectroscopy, ^{13}C-NMR spectroscopy, and FT-IR spectroscopy. Epoxy films were then prepared by reacting ferrocene carboxylic acid (10, 15, and 20% by wt) with bisphenol A diglycidyl ether followed by thermal setting of thin films using m-phenylene diamine. Epoxy thin films were tested via a standard burn test and thermogravimetric analysis. Additionally, differential scanning calorimetry was also utilized to study the thermal transitions of the prepared films. Thin films were also prepared with ferrocene carboxylic acid and triphenylphosphine oxide to determine the potential synergistic effects.

TABLE OF CONTENTS

CHAPTER PAGE

LIST OF TABLES

TABLE PAGE

LIST OF FIGURES

FIGURE PAGE

LIST OF ABBREVIATIONS

FR- Flame retardant

^{1}H NMR- Proton nuclear magnetic resonance

^{13}C NMR- Nuclear magnetic resonance

FT-IR- Fourier-transform infrared spectroscopy

FCA- Ferrocene carboxylic acid

BA- Benzoic acid

BADGE- Bisphenol A diglycidyl ether

TBAB- Tetrabutylammonium bromide

TPPO- Triphenylphosphine oxide

TGA- Thermogravimetric analysis

DSC- Differential scanning calorimetry

CHAPTER I

INTRODUCTION

1.1 Polymer Flame Retardant

Currently, the demand for polymer materials is significantly increasing whether natural or industrial. Since many polymers are flammable, significant damage can result upon their combustion. To avoid these risks, flame retardants are required to decrease toxic gases and smoke effects upon combustion. The development of polymer materials and flame retardants are required for commercial products to be safe when used. These flame retardant products are being used in various applications such as electrical, electronic, and building construction[1].

1.2 Flame Retardants

Flame retardants are substances that prevent fires from starting or lower the rate of spreading. These substances may offer more escape time and more safety. Flame retardants refer to function and not group or family of chemicals. A diverse molecular structures of chemistries and properties are used as flame retardants. Most of these chemicals are combined to enhance the efficiency of the process. The application of a flame retardant is useful since much electronic and electrical equipment are used when developing buildings. Reducing the combustibility rate of these materials helps decrease the risk of fire and results in the development of safer buildings. Also, these materials offers a beneficial layer

of protection which lowers the risk. Flame retardants have found wide application in three major areas including building materials, electrical and electronic devices, and transportation[2]. Table 1 illustrates the use of the flame retardant in the three major areas. The use of flame retardant in furnishings offers a protection layer and raises the escape time. When applied to trains, cars, and airplanes, these materials offer protection to passengers. In case of a crash, these materials hinder the ignition of fire or prevent the rate of spreading[3].

Table 1: Flame retardant market applications.

Market	***Group***	***FR requirements***
Building contents	Interior finishing, furnishings	Containment
Electrical and electronic	Electronic devices, wire and cable	Ignition resistance Flame spread
Transportation	Automobile, rail, aviation and aerospace	Escape time Containment

1.3 Conventional Flame Retardant and Toxicity

Since the 1970s, there has been a number of regulations which require commercial products to be safe under extreme temperatures and are nonflammable. This led to the development of halogenated FRs containing bromine or chlorine[4]. Considering the low cost and excellent performance of these FRs, they garner a significant share of the global market, as shown in **Figure 1**.

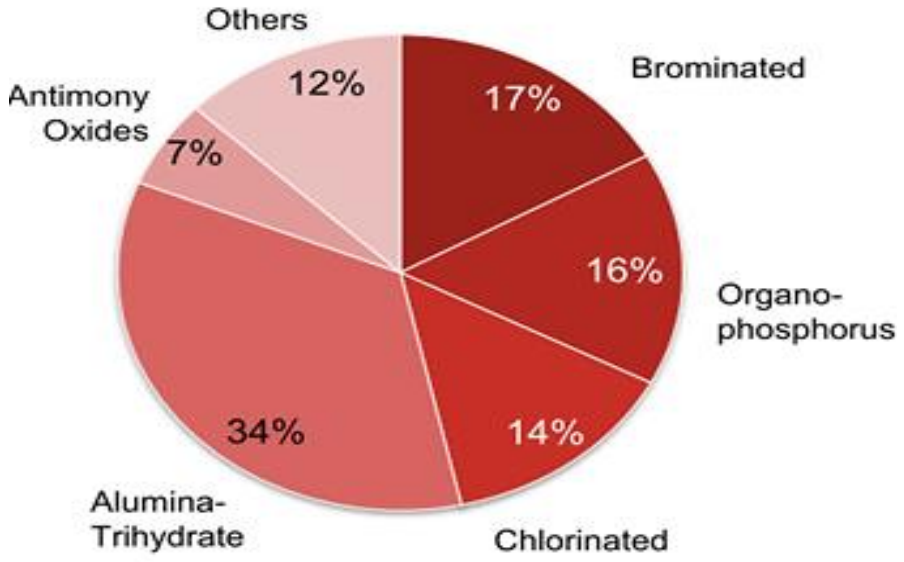

Figure 1: Halogenated and other FRs in the global production.

However new regulations were passed for FRs to lessen their impact on the environment. Examples include antimony trioxide and zinc which are toxic substances for the environment. The regulations were Restriction of Hazardous substances (RoHS) and Regulation on Registration, Evaluation, Authorization and Restriction of Chemicals declared these FRs as toxic and hazardous to the environment. As a result, researchers explored the use of alternative materials as effective FRs.

1.3.1 Phosphorus Based Flame Retardants

Phosphorus flame retardants need polymers that contain oxygen or nitrogen to show high performance. Many phosphorus-based FRs react with the polymer and add charring to separate the oxygen from the polymer; known as a condensed phase mechanism[5]. Some phosphorus-based FRs can vaporize into the flame to slow down the burning process.

However, these phosphorus compounds have a low boiling point and are often lost during processing.

1.3.2 Metal Hydroxides Flame Retardant

Metal hydroxides have high efficiency when they are used as FR. Metal hydroxides are used as FR because they are cheap and non-toxic to the environment. Upon combustion they decompose and convert to metal oxides and water through a highly endothermic reaction, which lowers the energy from the inflammation source. This heat sink mechanism refers to the resulting water evaporating that makes the polymer surface cooler and dilutes gases during combustion[6].

1.3.3 Melamine Polyphosphate,

Another alternative to halogens is melamine polyphosphate and it can simply be blended into polymers as a FR. Melamine polyphosphate has beneficial properties such as high thermal stability and low impact on the glass transition temperature. The melamine derivatives decompose to release nitrogen gases to reduce the amount of oxygen and any flammable gases[6]. Phosphoric acid can also produce char to isolate the polymer from oxygen. **Figure 2** shows the chemical structure of MPP.

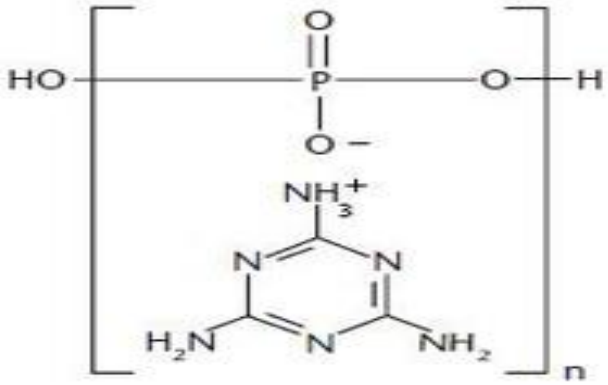

Figure 2: Melamine polyphosphate (MPP) structure.

1.4 Epoxy Resins

An epoxy resin is a thermosetting polymer. The term 'epoxy' is often referred to as a chemical group consisting of oxygen bonded to two carbons[7], as shown in the **Figure 3**. Epoxy resins generally outperform many of the other resin types because of their improved mechanical properties and resistance to aging. They are mostly used in applications like adhesives, coatings, and composite materials[8].

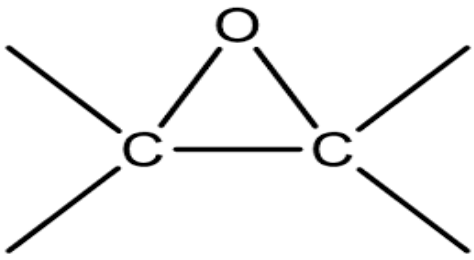

Figure 3: Epoxy group structure.

Like other thermosetting polymers, epoxy resins undergo decomposition by releasing soot, smoke, and toxic compounds, when exposed to temperatures in excess of 300°C[9]. To improve their flame retardancy, FRs are commonly reacted into the polymer. This approach not only improves the flame-retardant properties, but also maintains original physical and mechanical properties. Phosphorus-based compounds are commonly added to epoxy resins using this approach[10]. A variety of research studies have reported the modification of flame resistant properties of epoxy resins by using phosphorus-based compounds [1,6].

Epoxy resins have also been incorporated with silicon-containing glycidyl monomers and the fire-retardant properties were studied. It was found that oxidation temperatures were increased, and char formation was enhanced at high temperatures [11, 12]. Recently, a flame retardant containing phosphorus, nitrogen, and boron, was synthesized and blended with bisphenol-A diglycidyl ether to produce a flame-retardant epoxy resin. The resultant epoxy resin showed an improvement of 35.6% in the limited oxygen index and reduction in the smoke formation[13].

1.5 Ferrocene Flame Retardants

Ferrocene is an important organometallic compound having a sandwich-like structure. As shown in the **Figure 4**, the iron atom is between two parallel cyclopentadienyl rings. It was discovered in 1951 and the first polymer having a ferrocene unit in its main chain was reported in the year 1970 [14, 15].

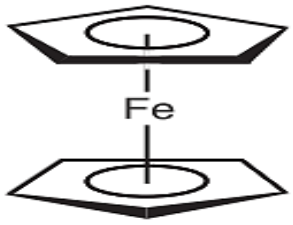

Figure 4: Ferrocene structure.

The introduction of ferrocene in the 20th century resulted in significant changes to organometallic chemistry. In present, it is applied in many areas including medicine, manufacturing, and technology. In addition, the incorporation of organometallic units into polymeric structures has made significant impacts on various fields due to the behavior and nature of the involved metal. The discovery of organometallic polymers has initiated a shift in the area of organometallic chemistry. This is because the addition of metal atoms creates desirable properties which lead to improved processability.

1.6 Literature Review

The incorporation of ferrocene units into a polymer can give properties such as flame retardancy[16], reversible oxidation, and thermal stability [17, 19]. In addition, ferrocene-based thermosetting polymers can be effective as catalysts and functional coatings[22]. A new copolymer was developed in which ferrocene, benzene, and diamine groups were combined via an aza-Michael addition reaction. For example, ferrocene-based polyamides synthesized through condensation reaction exhibit improved heat and flame-resistant properties[20].The copolymer exhibited good flame retardancy and charring

characteristics[16]. Ferrocene moieties have influenced beneficial changes in the field of polymer chemistry particularly in polymer synthesis[23].

Ferrocene has been found to have synergistic flame-retardant effects and smoke suppression properties. Liu et. al., conducted research to determine the flame retardancy and smoke suppression properties of ferrocene. The outcome of the study revealed that incorporation of ferrocene in the intumescent flame-retardant epoxy resins composition tends to extensively lower the amount of heat and smoke released. The compound was also found to be effective in enhancing the structure of char residue. Some of the volatilized products in the thermal degradation process included carboxylic acid, CO, H_2O, and aliphatic hydrocarbons. This indicated that ferrocene is effective in suppressing smoke. It also has an effective synergism[24].

Flame retardant polyurethanes have found wide usage for both industrial and commercial purposes. A recent study conducted by Giffin (2016) synthesized ferrocene derivatives with multiple hydroxyl groups in order to use them in a polyurethane thin film. The study synthesized di-(2,3 dihydroxypropyl) ferrocene 1-1'-dicarboxylate[25]. In addition, Zhang et. al., has used ferrocene derivatives medicinally. "Ferroquine" is the drug that has been clinically tried as an antimalarial[26].

Ferrocene as a flame retardant incorporated in epoxide takes several mechanisms. Usually, in the poisoning/vapor phase some gas is generated that is denser than oxygen. The process of generating the gases eliminate the fire by displacing the oxygen. It also leads to reduce the flame temperature. In addition, after the burning takes place, char is formed which works as an insulation barrier between the residual material and flame. The process further obstructs the flame from accessing the oxygen[27].

1.7 Project Rationale

Current literature shows that a majority of research studies have focused on the structural[28, 29] and electrochemical properties of ferrocene. However, research studies focusing on the flame retardant or thermal properties of the ferrocene incorporated epoxies are scarce[16]. Considering these findings, the present study has investigated the fire-resistant properties of epoxies incorporated with ferrocene moieties to reduce flammability.

Halogenated FR are environmentally hazardous and produce toxic smoke. Ferrocene is a good alternative to halogenated FR. However, ferrocene has a high vapor pressure, which may result in sublimation. To solve this problem, ferrocene was chemically bonded into epoxies.

Ferrocene carboxylic acid was attached to bisphenol A diglycidal ether followed by curing with m-phenylene diamine. In addition, triphenylphosphine oxide was incorporated to determine potential synergistic effects between it and the ferrocene. The synthesized epoxies were characterized using Fourier-Transform Infrared Spectroscopy (FTIR) and thermal characteristics were studied by using Thermogravimetric Analysis (TGA), a burn test, along with differential scanning calorimetry (DSC).

CHAPTER II

EXPERIMENTAL

2.1 Materials

All materials were commercially available and used without further purification unless otherwise stated. Ferrocene carboxylic acid was prepared using a literature method[30]. Epoxy thin films were prepared from bisphenol A diglycidal ether (BADGE), using m-phenylene diamine (MPDA) for curing.

2.2 Characterization

^{1}H-NMR and ^{13}C-NMR spectra were obtained using a Bruker Ultrashield™ 300 MHz Nuclear Magnetic Resonance spectrometer. FT-IR spectra were obtained with a Perkin-Elmer Spectrum Two™ Fourier Transform Infrared (FT-IR) L1600400 spectrometer. A standard burn test was performed in a vertical flame chamber. The TGA was performed with a TGA- Q50, and the DSC was performed with DSC-Q100 both from TA instruments.

2.3 Synthesis of Ferrocene Carboxylic Acid

Ferrocene (10.46g, 0.056 mol) and 2-chlorobenzoyl chloride (175 mol) were dissolved into dichloromethane (115 ml) in a flask. The sample was cooled in an ice bath followed by the addition of aluminum chloride (7.86 g, 0.058 mol). The solution color changed from red to purple. The reaction was stirred in an ice bath for thirty minutes and

1 hour at room temperature. The solution was then added to ice water (300 mL) with stirring. The mixture was transferred to a separator funnel and the layers were separated. The aqueous layer was extracted with two (50 mL) portions of dichloromethane. The combined organic solution was extracted with water (50 mL) once and 10% aqueous potassium hydroxide. The organic solution was then dried with magnesium sulfate, filtered and evaporated to dryness. In the second step, to a round-bottomed flask was added 1,2-dimethoxyethane (250 mL), potassium tert-butoxide (46.0 g, 0.0089 mol) and water (0.12 mol). The resulting slurry was stirred followed by the addition of the crude (2-chlorobenzoyl) ferrocene under a N_2 atmosphere. After 1 hour, the reaction was poured into water (1,700 mL) and extracted with diethyl ether (3 x 150 mL). The diethyl ether layers were extracted with 10% aqueous potassium hydroxide (2 x 50 mL). The aqueous solution was acidified with concentrated hydrochloric acid. The precipitate was collected by suction filtration and dried under reduced pressure to give an 83 % yield of ferrocene carboxylic acid.

2.4 Casting of Thin Films

2.4.1 Epoxy Films Incorporated with Benzoic Acid

BADGE (4.00 g, 0.011 mol), benzoic acid (0.40 g, 0.0031 mol), and tetrabutylammonium bromide (0.080 g, 0.00024 mol) were mixed in a beaker and place in an oven at 80°C for 2 hours. After that, m-phenylene diamine (0.60 g, 0.0055 mol), was added to the mixture. The mixture was cast as a thin film onto a glass slide and placed back in the oven at 80°C for 2 hours. The heat was then increased to 150°C for 4 hours. Two additional films were also prepared with benzoic acid loadings of (0.60 g, 0.0049 mol) and

(0.80 g, 0.0056 mol). FT-IR spectrum showed absorbences at 3400, 3050, 2950, 1650 and 1100 cm^{-1}.

2.4.2 Epoxy Films Incorporated with Ferrocene Carboxylic Acid

BADGE (4.00 g, 0.011 mol), ferrocene carboxylic acid (0.40 g, 0.0017 mol), and tetrabutylammonium bromide (0.080 g, 0.00024 mol) were mixed and placed in an oven at 80°C for 2 hours. M-phenylene diamine (0.60 g, 0.0055 mol) was added to the mixture and thin films were cast on to a glass slide and placed back in the oven for two hours 80°C. The temperature was then raised to 150°C for 4 hours. The same thin film procedure was used FCA loadings of (0.60 g, 0.0026 mol) and (0.80 g, 0.0034 mol). FT-IR spectrum showed peaks at 3400, 3050, 2950, 1650 and 1100 cm^{-1}.

2.4.3 Epoxy Films Incorporated with Ferrocene Carboxylic Acid and Triphenylphosphine Oxide

BADGE (4.00 g, 0.0118 mol), ferrocene carboxylic acid (0.40 g, 0.0017 mol), tetrabutylammonium bromide (0.080 g, 0.00024 mol) and triphenylphosphine (0. 40g, 0.0015 mol) were mixed and placed oven at 80°C for two hours. M-phenylene diamine (0.60 g, 0.0055 mol) was added to the mixture and thin films were cast on to a glass slide and placed back in the oven for two hours 80°C. The temperature was then raised to 150°C for four hours. The same procedure was used FCA loadings (0.60 g, 0.0026 mol) and (0.80 g, 0.0034 mol). FT-IR spectrum showed peaks at 3400, 3050, 2950, 1650 and 1100 cm^{-1}.

CHAPTER III

RESULTS AND DISCUSSION

3.1 Synthesis of Ferrocene carboxylic acid

Ferrocene carboxylic acid was synthesized using a two-step process. Ferrocene reacted with 2-chlorobenzoyl chloride under Friedel-Crafts conditions. The benzoyl ferrocene was then hydrolyzed with water and potassium tert-butoxide. The overall yield of FCA was 83%. The synthesis of FCA is shown in **Figure 5**.

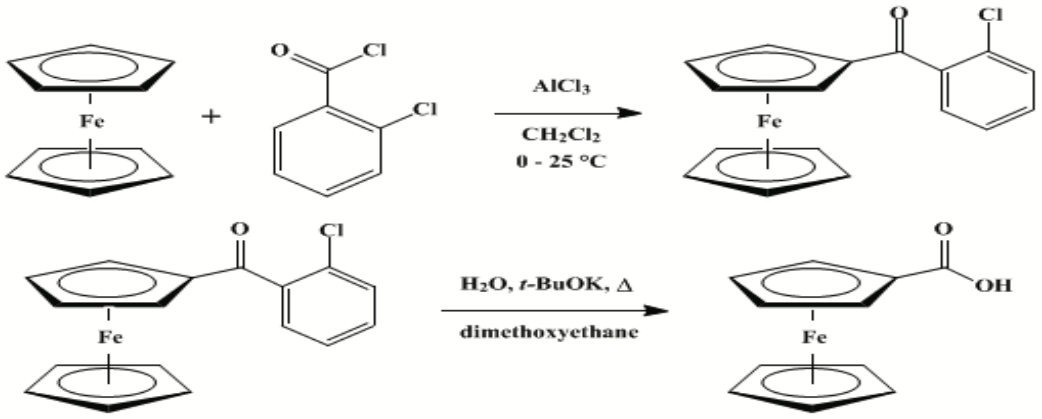

Figure 5: Schematic synthesis of FCA.

3.2 Monomer Characterizations

The molecular structure and purity, and the functional groups of the ferrocene, 2-chlorobenzoyl chloride, 2-chlorobenzoyl ferrocene, and ferrocene carboxylic acid were analyzed by ^{1}H-NMR, ^{13}C-NMR, and FT-IR spectroscopy.

3.2.1 ^{1}H-NMR, ^{13}C-NMR, and FT-IR Spectra of Ferrocene

Figures 6-8 show ^{1}H-NMR, ^{13}C-NMR, and FT-IR spectra of ferrocene. First, the ^{1}H-NMR spectrum of ferrocene was performed using $CDCl_3$ as the solvent. The ferrocene exhibited a peak at 4.2 ppm. This observed peak agreed with the standard ^{1}H-NMR of ferrocene according to SDBS [31]. Also, some peaks were observed in the area between 1.3 -1.6 ppm. These peaks can be indexed to a small amount of aliphatic impurities, as shown in **Figure 6**. Second, the ^{13}C-NMR spectrum of the ferrocene was also analyzed using the same solvent. The ^{13}C-NMR spectrum showed two peaks at 77.22 and 68 ppm. The two peaks refer to the $CDCl_3$ solvent and ferrocene, respectively. The standard ^{13}C-NMR spectrum of ferrocene is at 67.83 ppm, which was consistent with the observed peak of the ferrocene in this study indicating its high purity, as illustrated in **Figure 7**. Finally, **Figure 8** illustrates the vibrational spectrum of ferrocene. The infrared spectrum of ferrocene revealed absorbences at 3090 and 1410 cm^{-1}. These values correspond to sp^2 C-H and C=C, respectively.

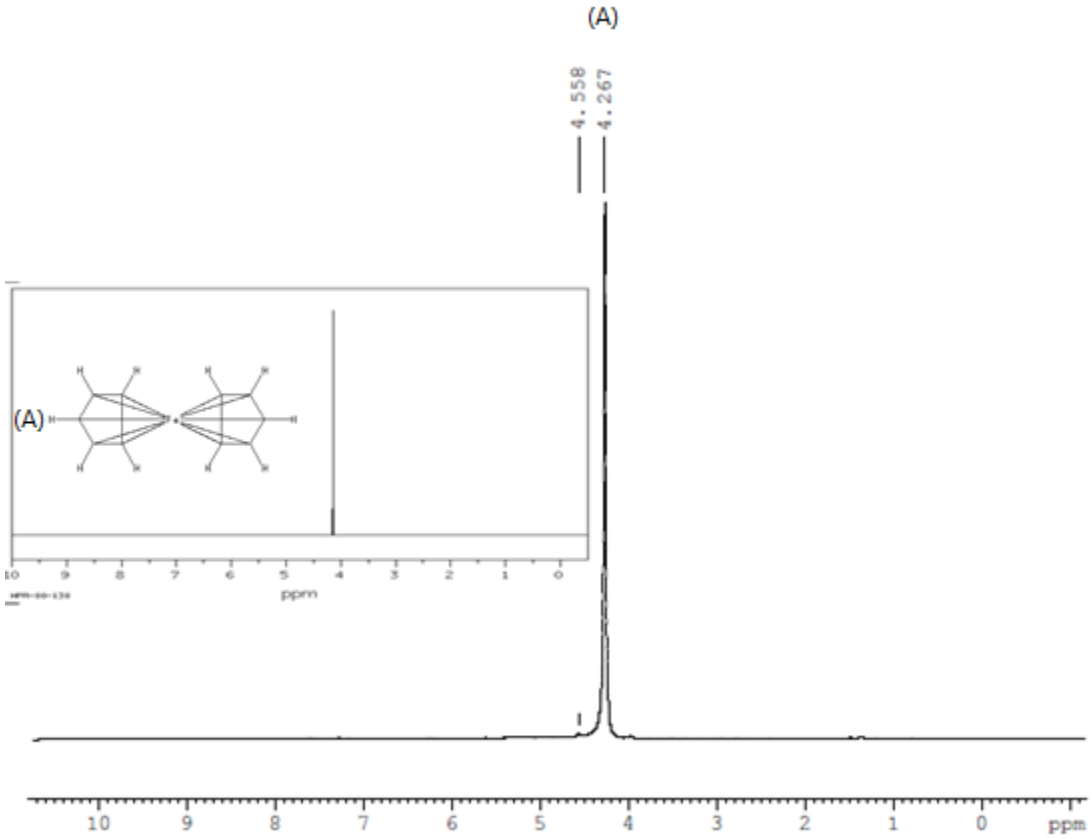

Figure 6: The ^{1}H-NMR spectrum of ferrocene with standard spectrum as inset.

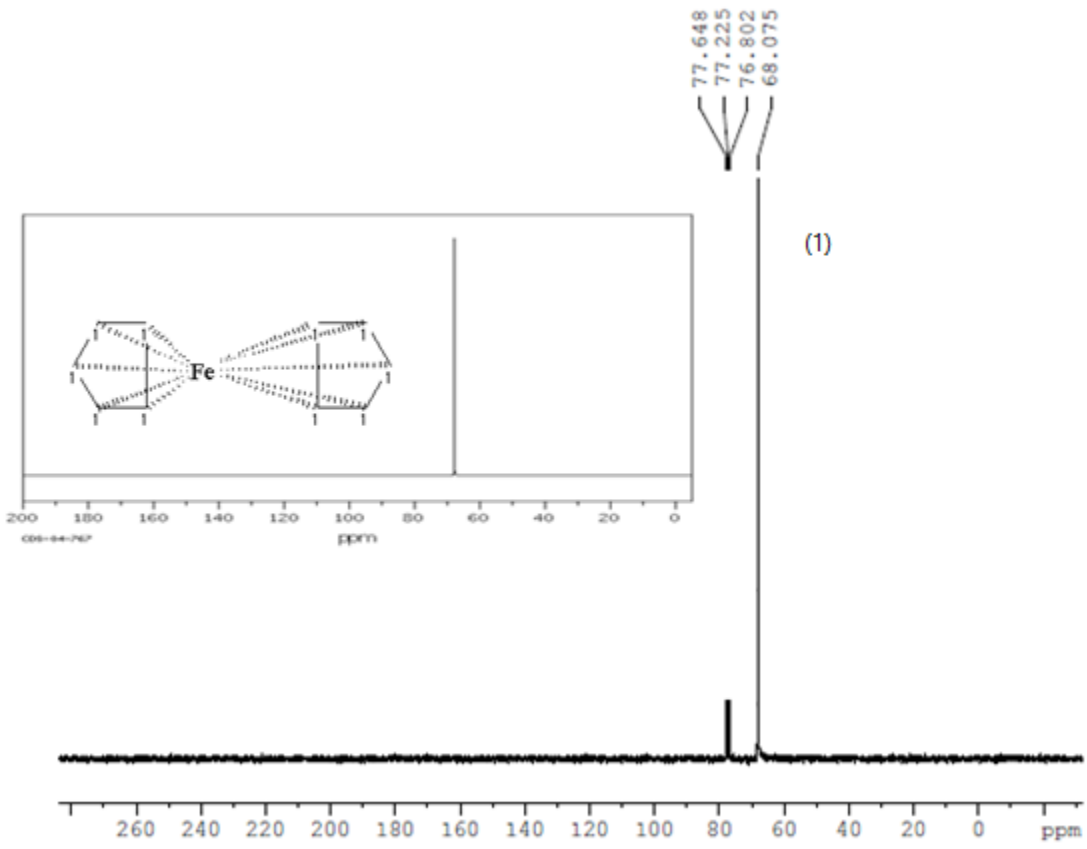

Figure 7: The ^{13}C-NMR spectrum of ferrocene with standard spectrum as inset.

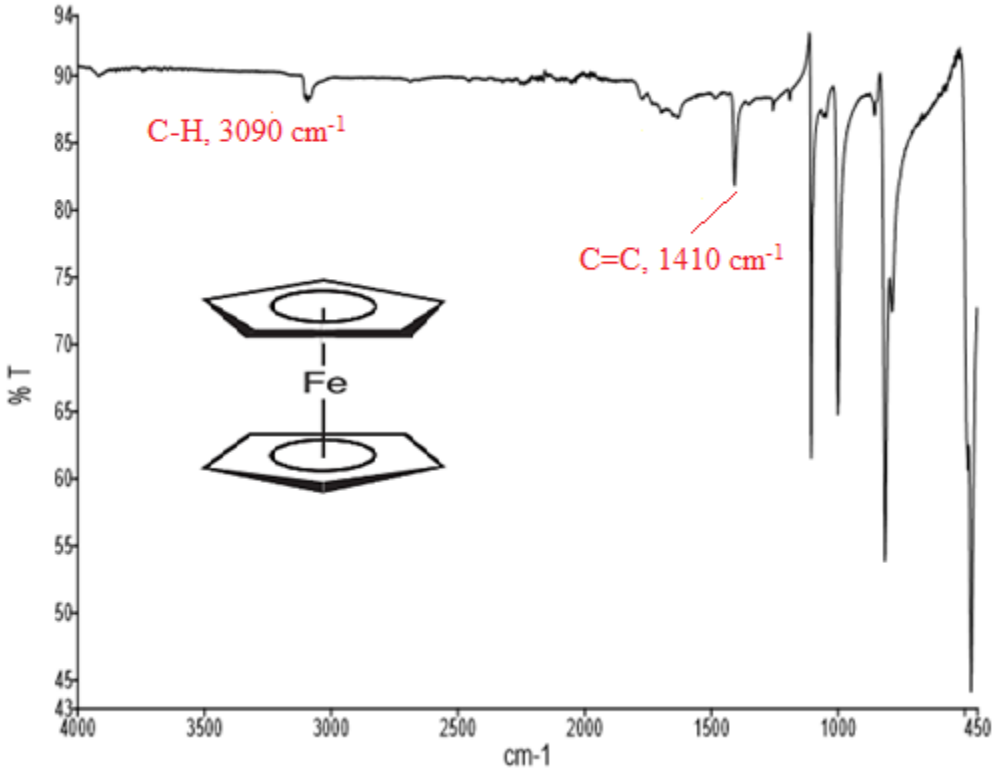

Figure 8: FR-IR spectrum of ferrocene.

3.2.2 ^{1}H-NMR, ^{13}C-NMR, and FT-IR Spectra of 2-Chlorobenzoyl Chloride

Figures 9-11 show ^{1}H-NMR, ^{13}C-NMR, and FT-IR spectra of 2-chlorobenzoyl chloride. The ^{1}H-NMR spectrum of 2-chlorobenzoyl chloride was accomplished using $CDCl_3$ as the solvent. The 2-chlorobenzoyl chloride showed three peaks at 7.48, 7.53, and 8.06 ppm. These peaks assign to 2-chlorobenzoyl chloride corresponding to meta, para, and ortho hydrogens. The standard peaks [31] of 2-chlorobenzoyl chloride appear at 7.49, 7.69, and 8.11 ppm, which is consistent to results as seen on **Figure 9**. In addition, the ^{13}C-NMR spectrum of the 2-chlorobenzoyl chloride was also investigated with $CDCl_3$ as the solvent. The ^{13}C-NMR spectrum exhibited six peaks at 77, 127, 131, 133, 135, and 166 ppm. These obtained peaks correspond to the solvent $CDCl_3$, meta, ortho, R, para, and carbonyl carbons. To compare with the standard 2-chlorobenzoyl chloride results, all the observed peaks matched well with the standard results, see **Figure 10**. **Figure 11** shows the vibrational spectrum of 2-chlorobenzoyl chloride. The FT-IR spectrum of 2-chlorobenzoyl chloride revealed absorbance at 3070, 1750, and 1600 cm^{-1} corresponding to sp^2 C-H, C=O, and C=C, respectively.

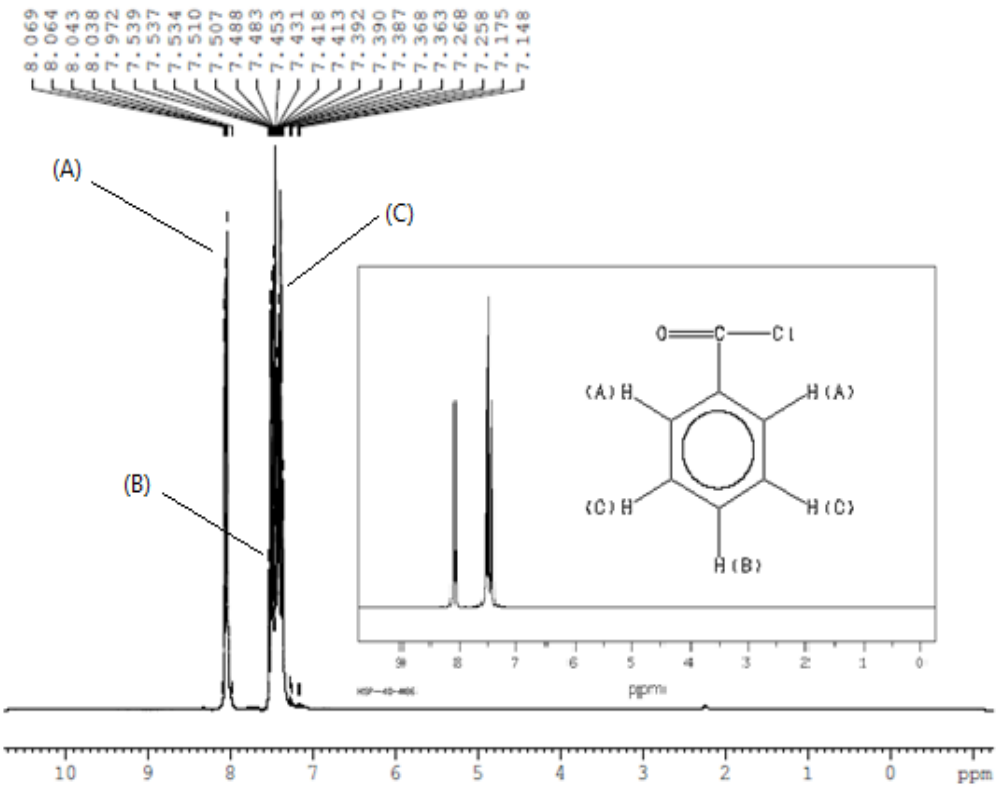

Figure 9: The ^{1}H-NMR spectrum of 2-chlorobenzoyl chloride with standard spectrum inset.

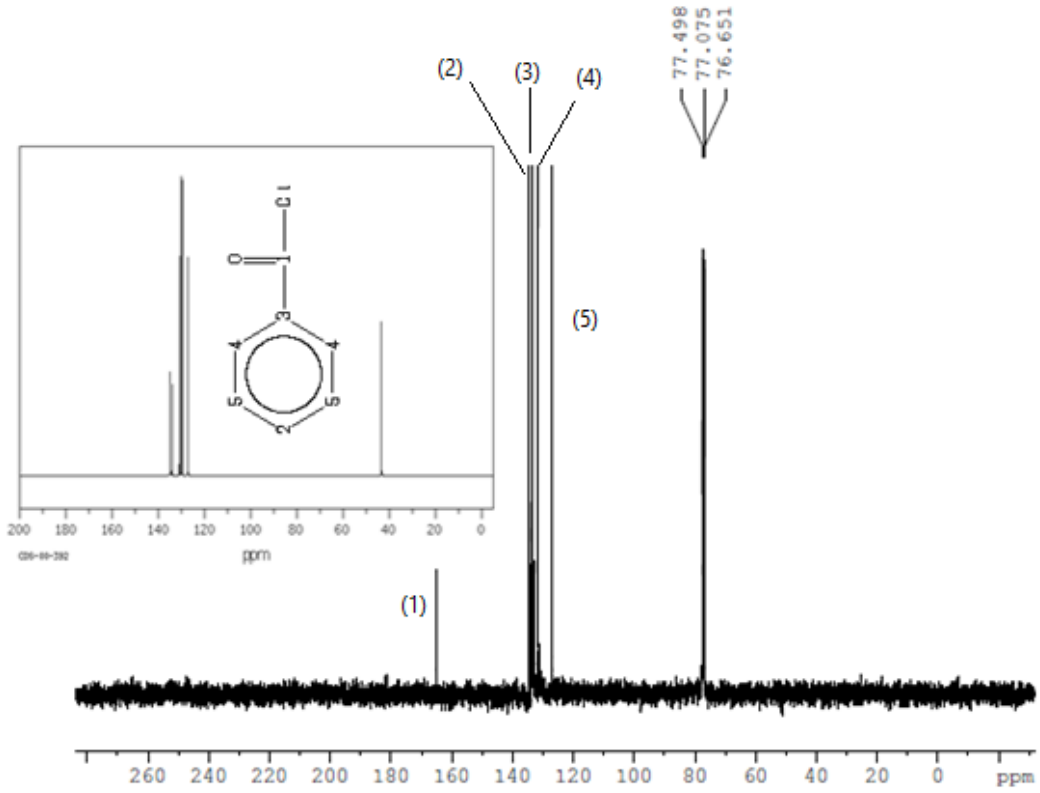

Figure 10: The ^{13}C-NMR spectrum of 2-chlorobenzoyl chloride with standard spectrum inset.

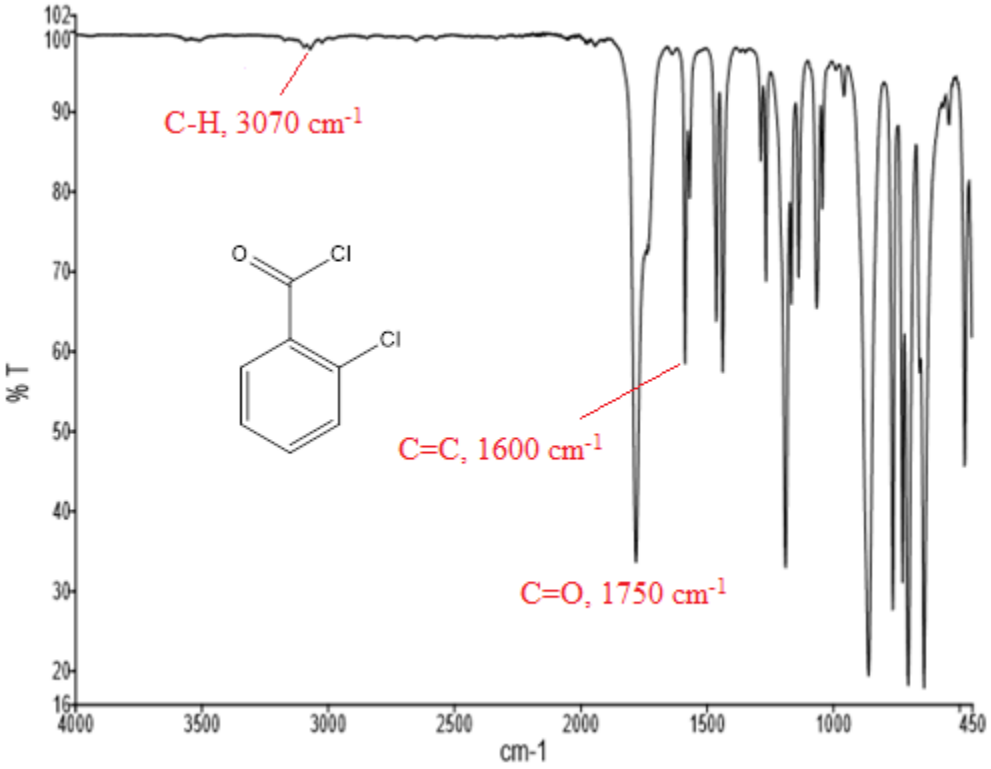

Figure 11: The FT-IR spectrum of 2-chlorobenzoyl chloride.

3.2.3 ^{1}H-NMR, ^{13}C-NMR, and FT-IR Spectra of 2-Chloro Benzoyl Ferrocene

Figures 12-14 show the ^{1}H-NMR, ^{13}C-NMR, and FT-IR spectra of 2-chloro benzoyl ferrocene. In the ^{1}H-NMR spectrum, four peaks were observed at 4.2, 4.7, 4.9, and 7.5ppm. These peaks correspond to the ferrocenyl protons (4.2, 4.7, and 4.9ppm) and the phenyl protons (7.5ppm) which was consistent with the reference spectrum. The ^{13}C-NMR spectrum of benzoyl ferrocene showed four peaks from 68 – 73ppm for the ferrocenyl protons, six peaks from 126 – 139ppm for the phenyl carbons, and a peak at 198ppm for the carbonyl carbon. This spectrum was consistent with the structure of o-chlorobenzoyl ferrocene. **Figure 14** shows the FT-IR spectrum of 2-chlorobenzoyl ferrocene with the peaks at 3090 and 1628 cm^{-1} that represents the sp^2 C-H and C=O stretching.

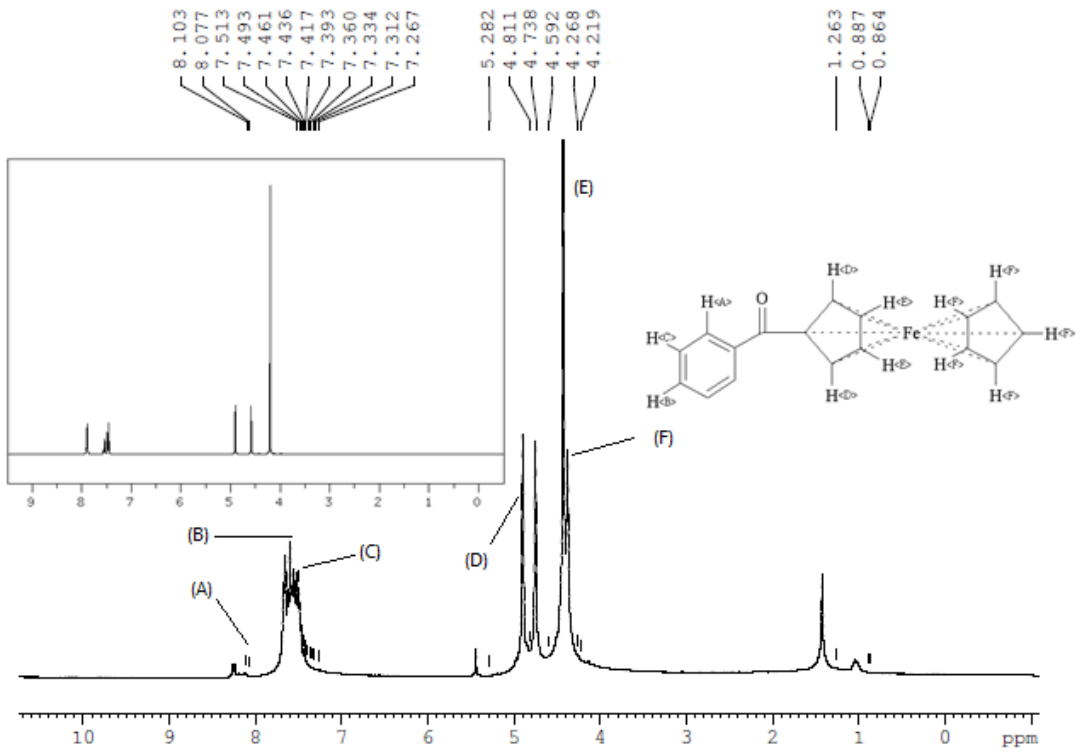

Figure 12: ^{1}H-NMR spectrum of 2-chlorobenzoyl ferrocene with reference spectrum inset.

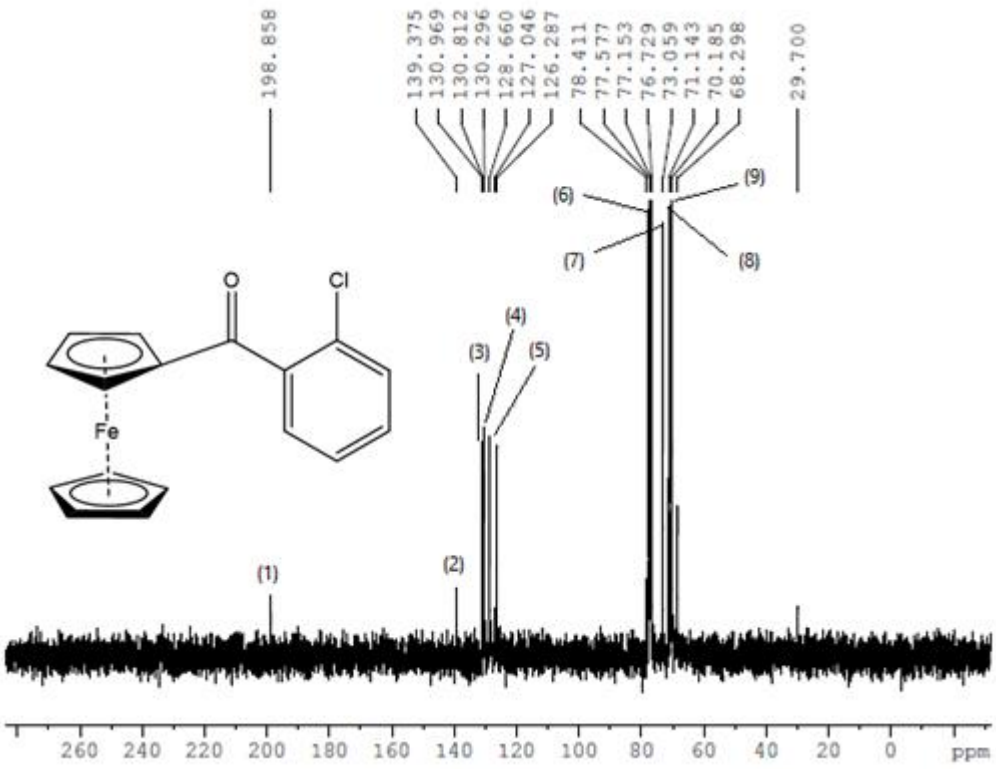

Figure 13: ^{1}H-NMR spectrum of 2-chlorobenzoyl ferrocene.

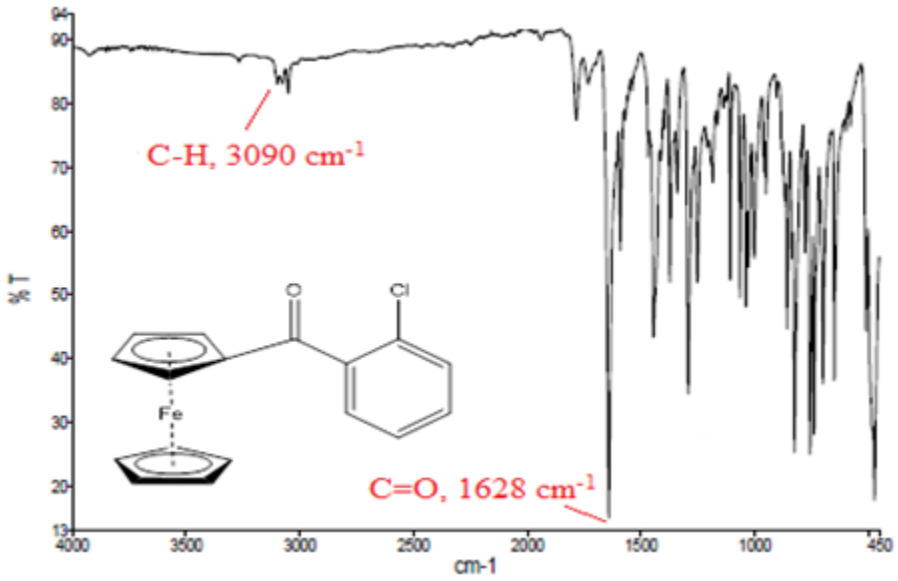

Figure 14: FT-IR spectrum of 2-chlorobenzoyl ferrocene.

3.2.4 ^{1}H-NMR, ^{13}C-NMR, and FT-IR Spectra of Ferrocene Carboxylic Acid

Figures 15-17 show ^{1}H-NMR, ^{13}C-NMR, and FT-IR spectra of ferrocene carboxylic acid. The ^{1}H-NMR spectrum of the ferrocene carboxylic acid was achieved using DMSO-d_6 as a solvent and showed four peaks at 2.5, 4.2, 4.4, and 4.7 ppm. The first two peaks can be attributed to the solvent dimethyl sulfoxide and the unsubstituted ferrocenyl ring while the last two peaks referred to a substituted ferrocenyl ring. Additionally, some peaks were observed in the area between 1.11 -1.59 ppm. These peaks can be indexed to a small amount of aliphatic impurities. However, the signal for the carboxylic acid proton at 8.6 ppm was not observed on the synthesized ferrocene carboxylic acid as seen in **Figure 15**. This may be due to severe broadening of the signal. Using the same solvent of DMSO-d_6 the ^{13}C-NMR spectrum of the ferrocene carboxylic acid was further analyzed, as seen in **Figure 16**. The ^{13}C-NMR spectrum exhibited four peaks from 70-72ppm for the ferrocenyl protons and a peak at 172ppm for the carbonyl carbon. The obtained ^{13}C-NMR spectrum of ferrocene carboxylic acid agreed well with the standard reference. Finally, the vibrational spectrum of ferrocene carboxylic acid was characterized via FT-IR. The IR spectrum revealed absorbencies at 3300-2500, 1650, and 1410 cm^{-1} referring to O-H, C=O, and C=C, respectively, as shown in **Figure 17**.

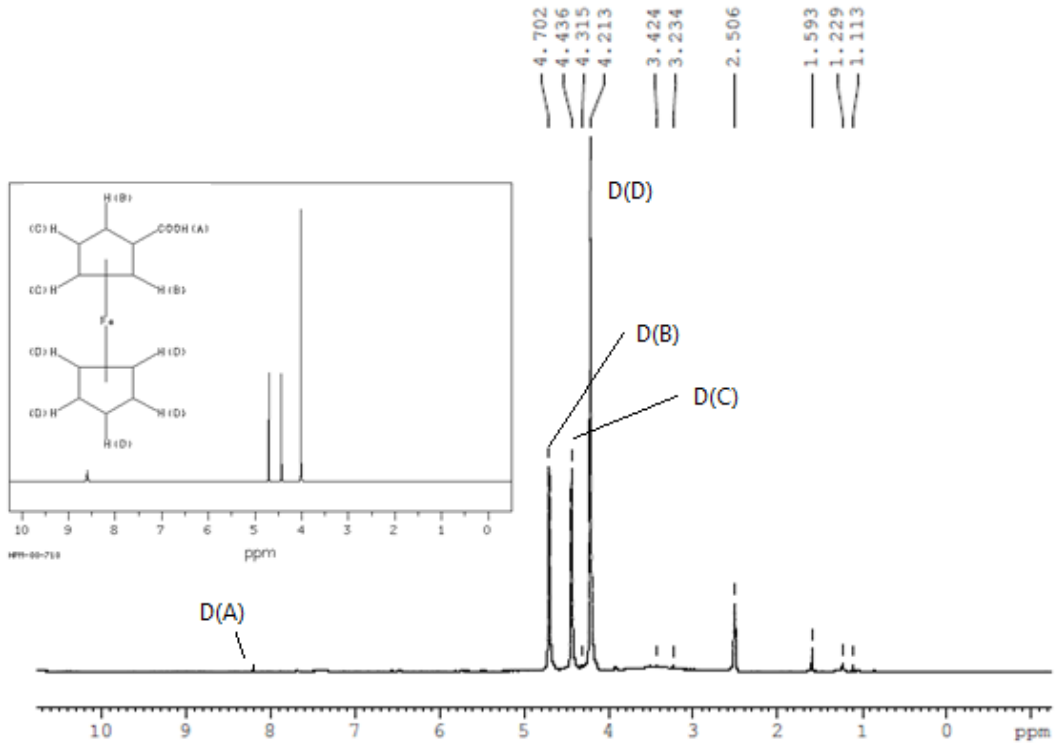

Figure 15: The ^{1}H-NMR spectrum of ferrocene carboxylic acid with reference spectrum as inset.

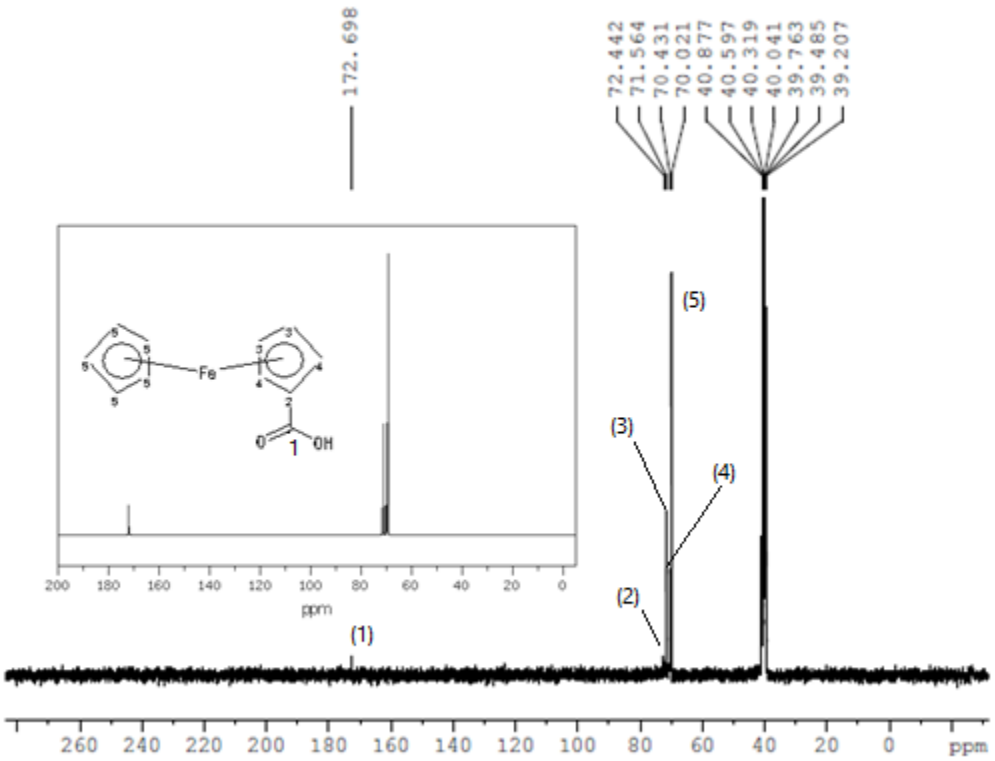

Figure 16: The ^{13}C-NMR spectrum of ferrocene carboxylic acid with reference spectrum as inset.

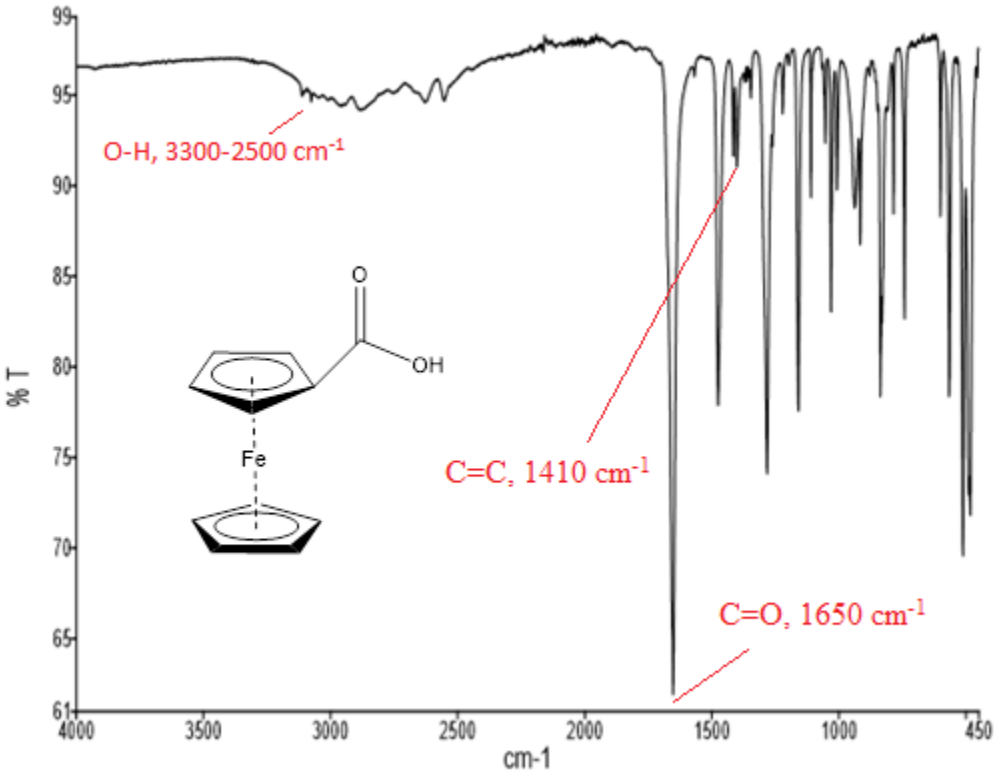

Figure 17: The FT-IR spectrum of ferrocene carboxylic acid.

3.3 Synthesis of Epoxide Films

The synthesis of epoxy films with FCA or BA was accomplished in two steps as illustrated in **Figure 18**. FCA was attached in various ratios (10, 15, and 20% by wt.) to the epoxy using tetrabutylammonium bromide as the catalyst at 80ºC. The solution was then cooled to room temperature and m-phenylene diamine was added and mixed. The mixture was poured onto a glass slide and thermally set. The FT-IR spectrum showed absorbencies at 3400, 2950, 1650, and 1100 cm^{-1}. The absorbencies correspond to an O-H, sp^3 C-H, C=O, and C-O, respectively. These were consistent with the structure of the epoxide film. FT-IR spectra of films with BA, FCA, and FCA+TPPO are shown in **Figures 19-21**.

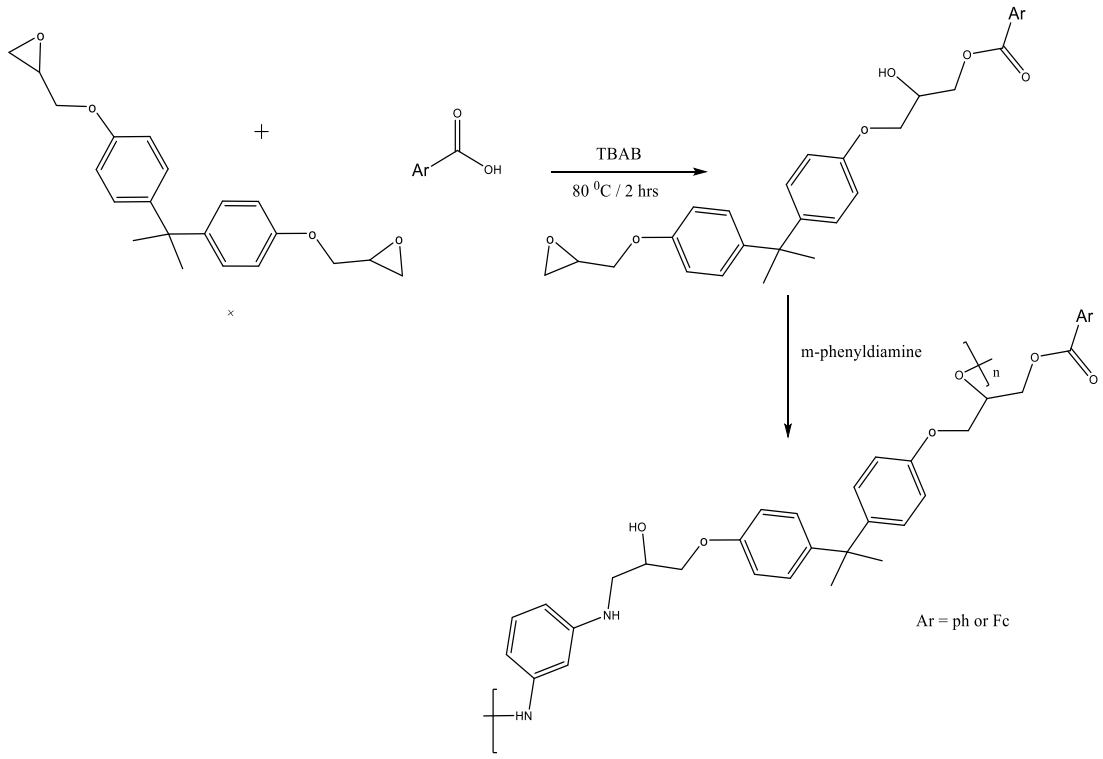

Figure 18: Schematic scheme of epoxy films with carboxylic acids.

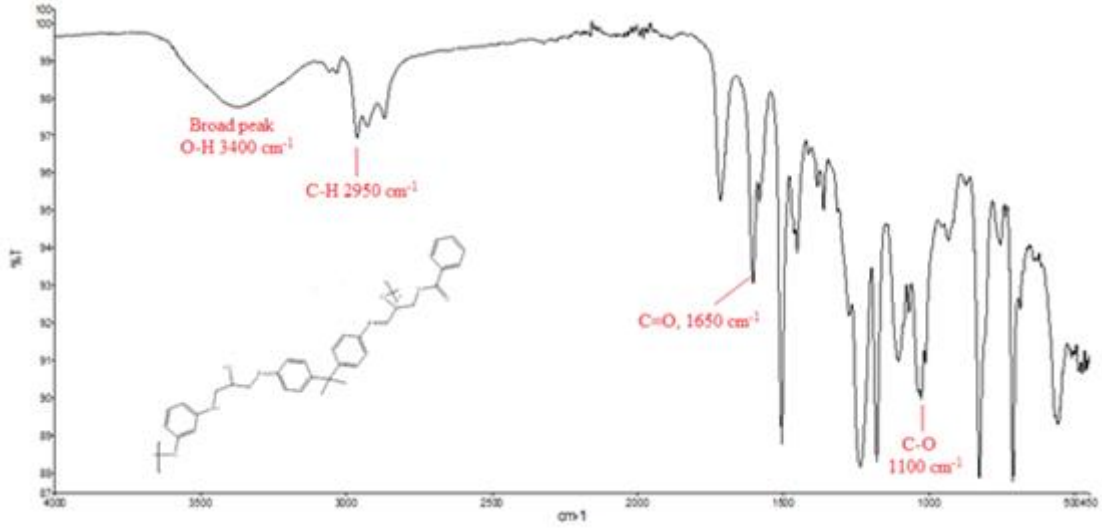

Figure 19: FT-IR spectrum of epoxy films incorporated with benzoic acid.

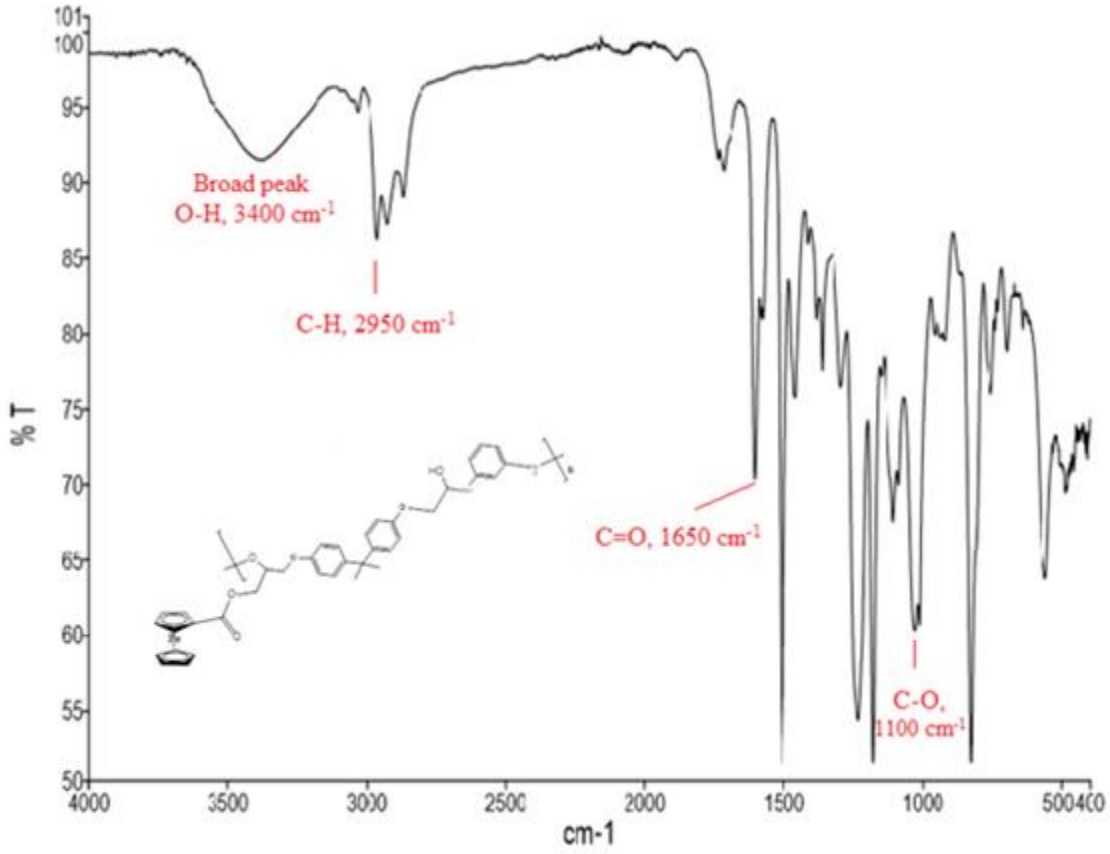

Figure 20: FT-IR spectrum of epoxy films incorporated with ferrocene carboxylic acid.

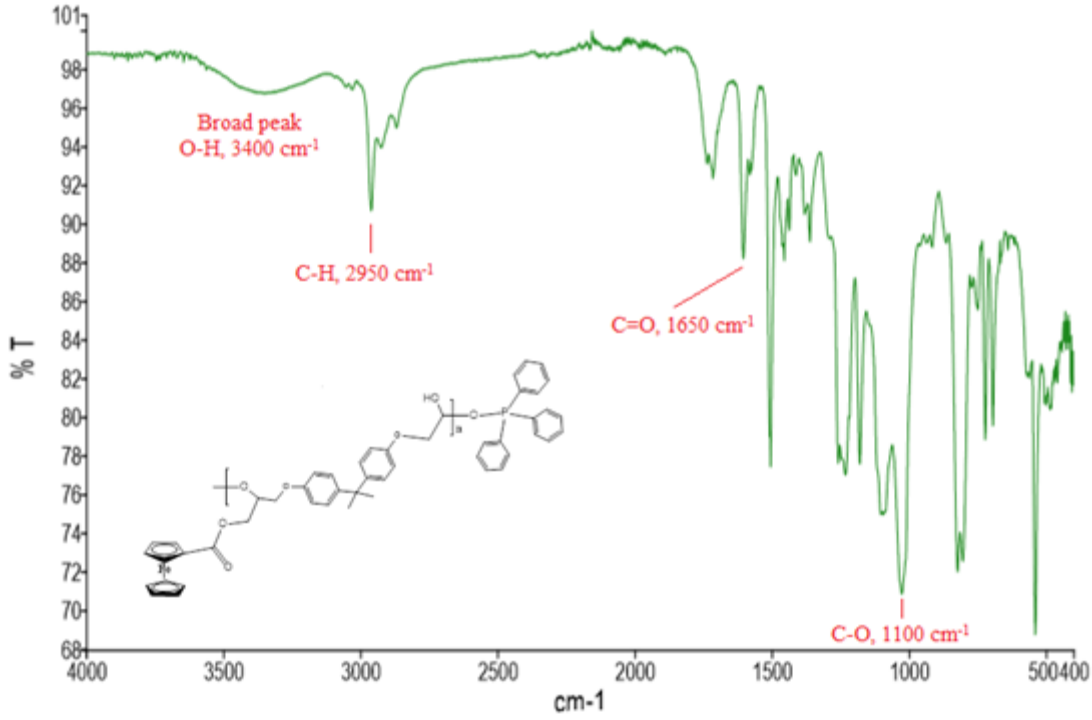

Figure 21: FT-IR spectrum of epoxy film incorporated with ferrocene carboxylic acid and triphenylphosphine oxide.

3.4 Thermal Properties

3.4.1 TGA Test

Thermogravimetric analysis (TGA) measures the weight loss of a sample versus increasing temperature at a constant rate. The temperature for this study ranged from 25 - 600 ^{o}C and the rate was 10^{o}C/min. Thermal stability of each polymer was determined at 10% weight loss and char yields were determined at 600^{o}C. The results of the TGAs are shown in **Table 2**.

Table 2: Temperature and 10 % weight loss with residue %.

Epoxy films	Wt % of acid	Temperature@10 % weight loss	Residue (%)
Benzoic Acid	10 15 20	325	17-19
FCA & FCA+TPPO	10 15 20	305	12-25

For benzoic acid containing epoxides, **Figure 22**, 10% weight loss was observed at approximately 325 ^{o}C for each sample and char yields ranged from 17 – 19%. There results were typical for an epoxide film and indicated the benzoic acid was not significantly affecting the thermal stability.

The TGA of epoxides incorporated with FCA and FCA+TPPO **Figures 23 and 24** showed thermal stabilities at approximately 305 ^{o}C with char yields ranging from 12 to 25%. These data showed a slightly less thermal stability than films with BA. However, the

thermal stabilities were only slightly lower and suggested the FCA did not significantly affect thermal stability.

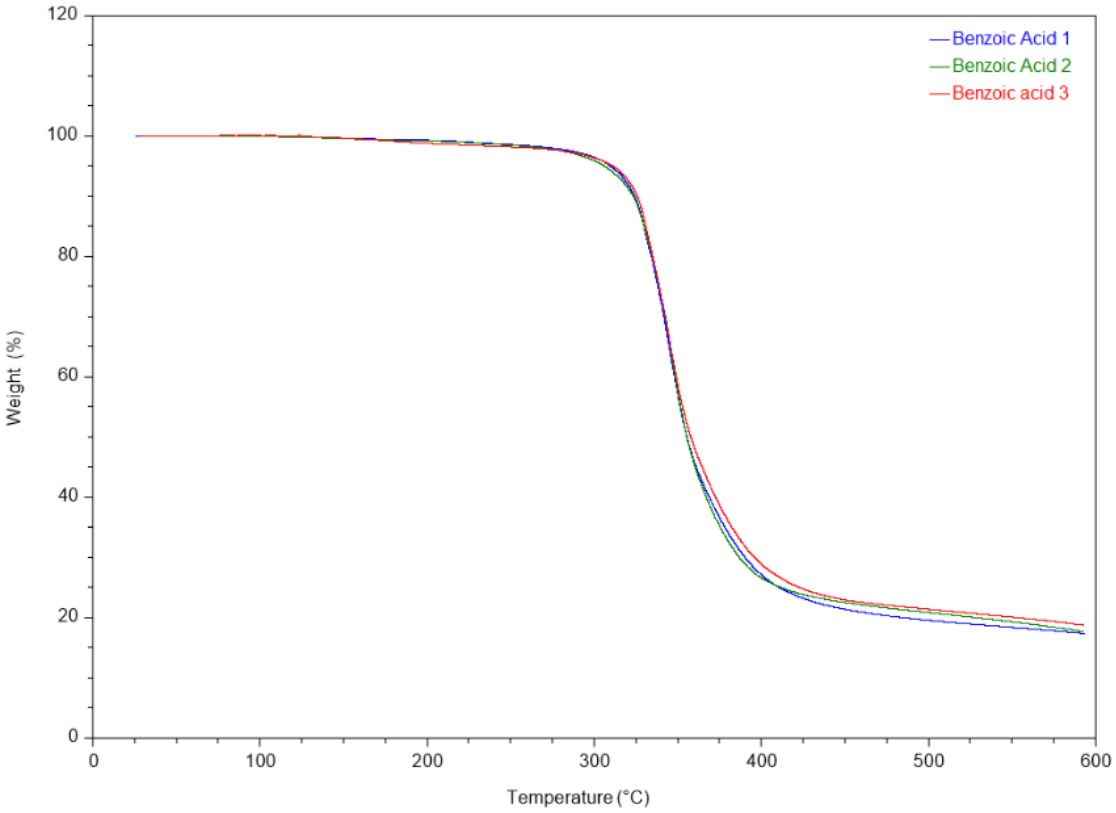

Figure 22: TGA of epoxy films incorporated with benzoic acid.

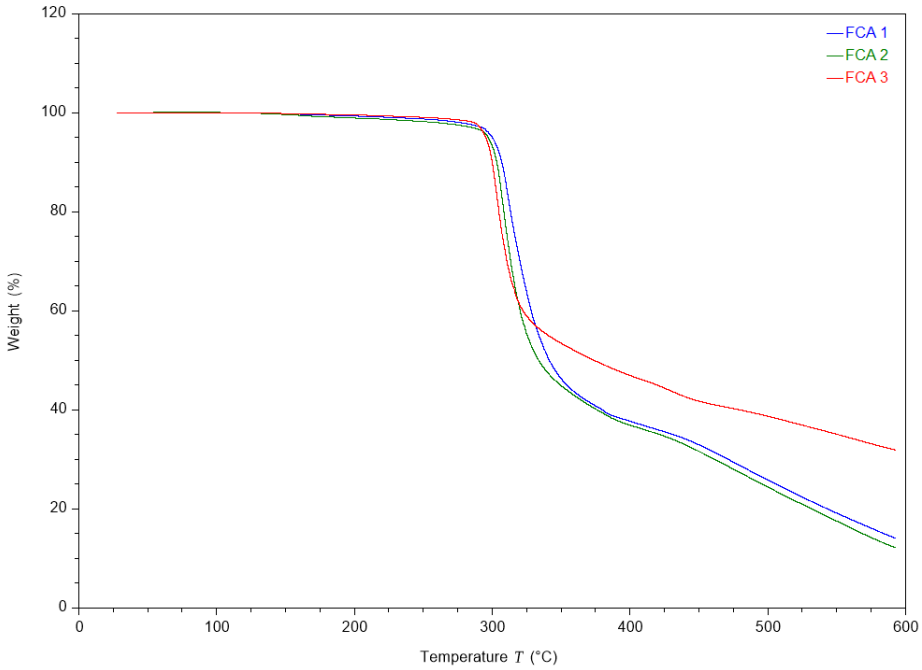

Figure 23: TGA of epoxy films incorporated with FCA.

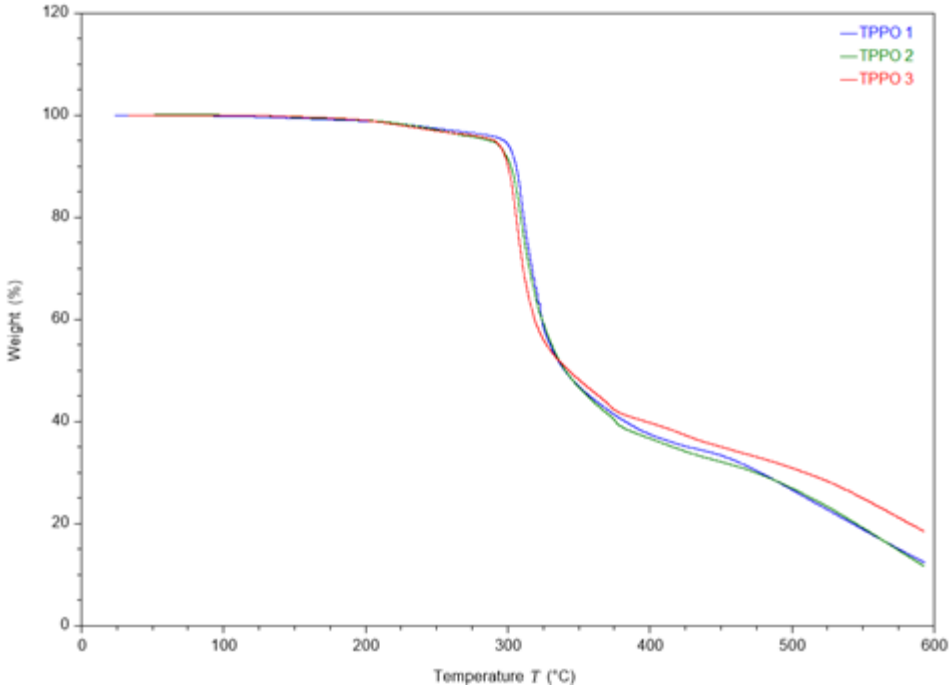

Figure 24: TGA data of epoxy film incorporated with FCA& TPPO.

3.4.2 DSC Test

Differential scanning calorimetry analysis (DSC) is a technique that is utilized to measure the thermal transitions of a polymer when it is heated such as a glass transition temperature (Tg), a polymer's crystallization temperature (Tc), and a melting point (Tm). Typically, the DSC analysis measures the quantity of heat absorbed by a sample and a reference then record the difference of temperature as a function of heat flow, as seen in **Figure 25 and 26**.

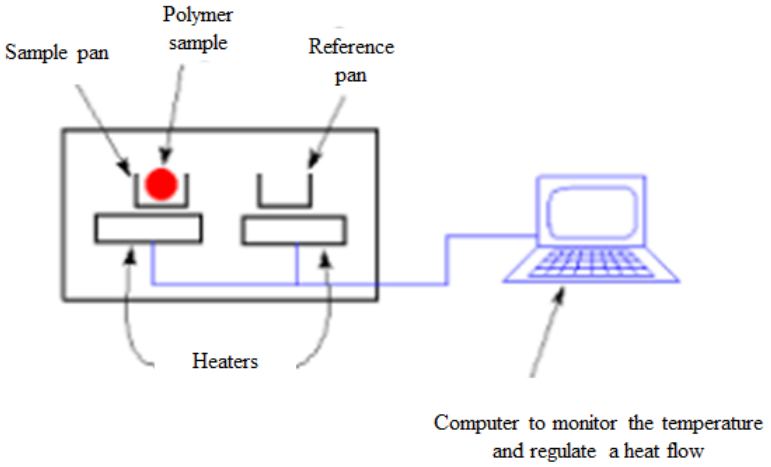

Figure 25: Differential scanning calorimetry schematic diagram.

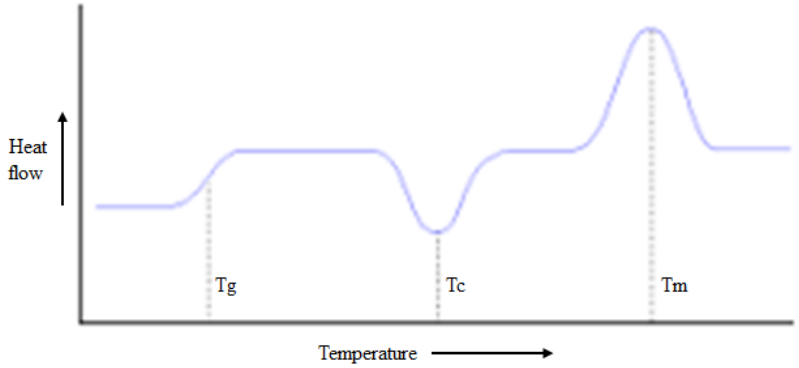

Figure 26: A typical DSC plot.

The differential scanning calorimetry measurements of epoxide thin films (benzoic acid, ferrocene carboxylic acid, and ferrocene carboxylic acid + TPPO) at a loading of 20% were performed. The thermal transitions of the epoxide films were determined via heating and cooling at the range of 25 – 250°C.

Graphs with BA, FCA, and FCA+TPPO are shown in **Figures 27, 28, and 29,** respectively. The epoxide film with BA showed a glass transition temperature of 85°C. The Tg of this material is slightly lower than the reported Tg of 95°C and may be due to less crosslinking [32]. In contrast, films with FCA and FCA+TPPO exhibited Tgs of 100 and 105°C, respectively. These results suggest a greater molecular organization within the epoxide resulting in a higher Tg.

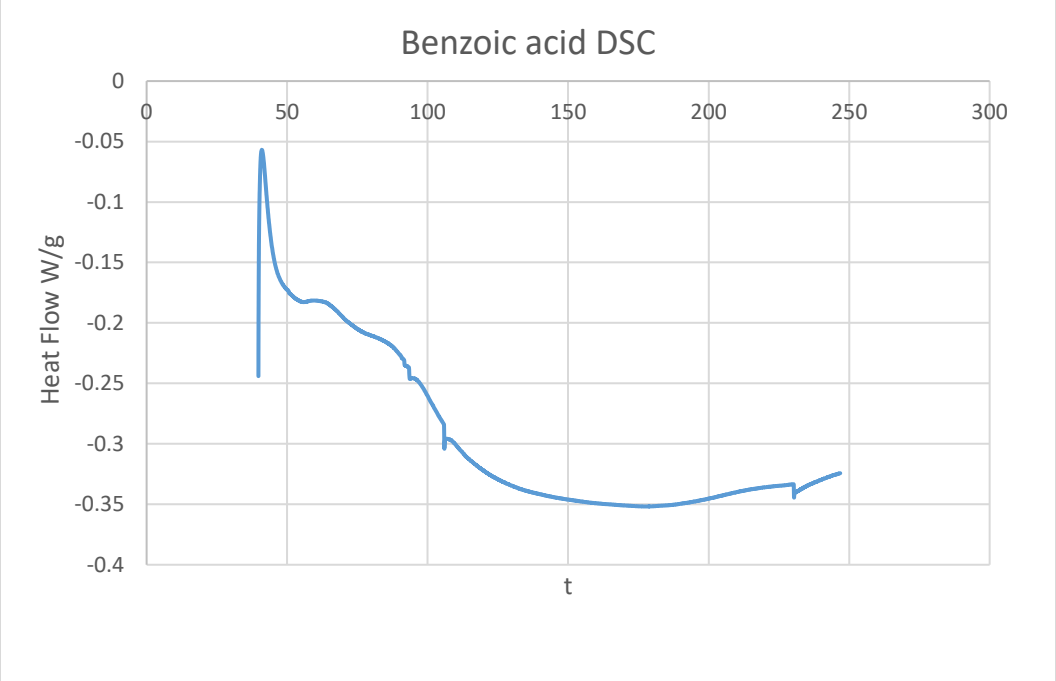

Figure 27: DSC data of epoxy film incorporated with benzoic acid.

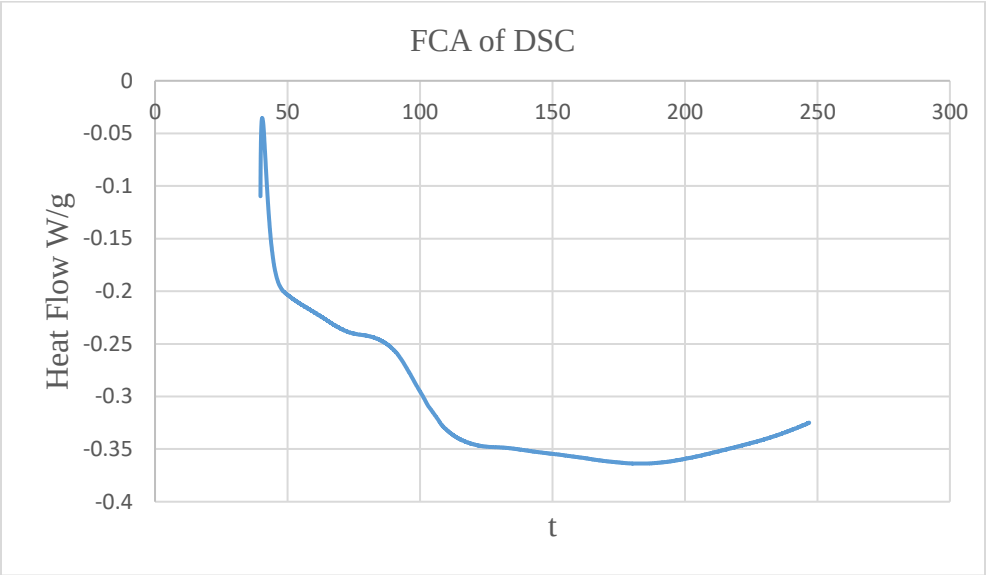

Figure 28: DSC data of epoxy film incorporated with FCA.

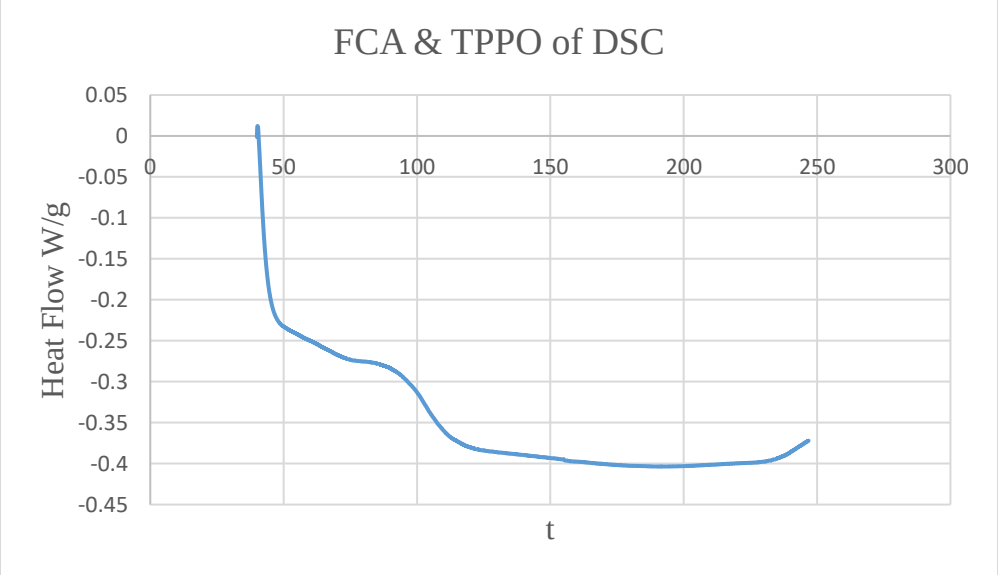

Figure 29: DSC data of epoxy film incorporated with FCA+TPPO.

3.4.3 Burn Test

Burn tests were completed on thin films of each epoxide. Each film was ignited by placing a Bunsen burner at the end of the film for 10 seconds according to the standard method for a burring test. The burn time and burn distance were then recorded as seen in **Figure 30 and Table 3**, respectively.

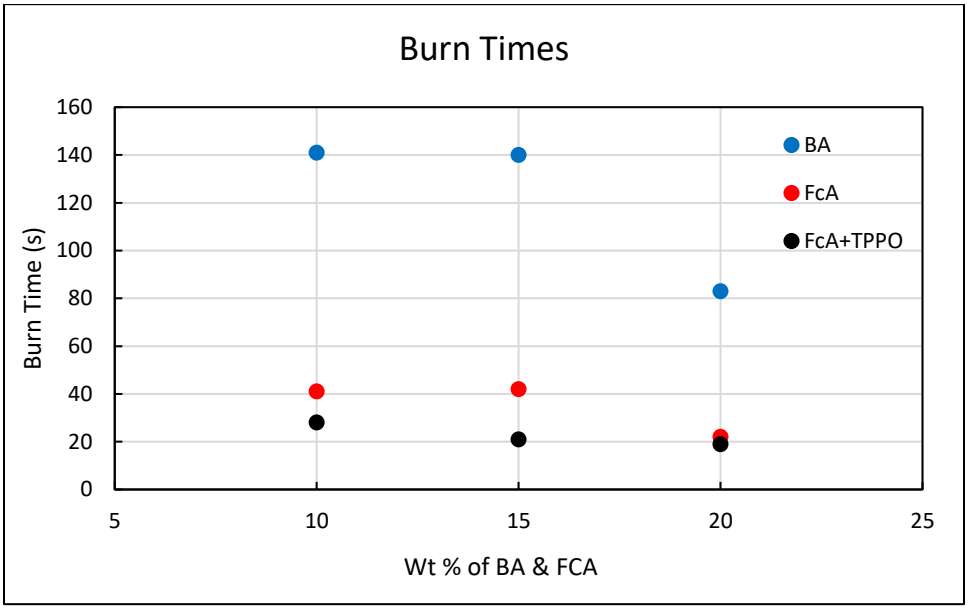

Figure 30: Burn rate versus wt % BA, FCA, & FCA+TPPO.

Epoxide films with BA showed burn times ranging from 82 to 140 s with burn distances of approximately 0.5 in. In contrast samples with FCA and FCA+TPPO exhibited much shorter burn times, 20-40 s, and significantly less burn distances of approximately 0.1 in. These results showed that films with ferrocene exhibited much less flammability and have the potential as FRs in epoxide films. Images of films before and after burning for BA, FCA, and FCA+TPPO are shown in **Figures 31, 32, and 33.**

Table 3: Burn distance vs. % BA, FCA+TPPO.

Sample	Ratio	Initial length (in)	Length after combustion (in)	Final length (in)
BA	10	3.1	2.5	0.6
	15	2.7	2.0	0.7
	20	2.3	1.8	0.5
FCA	10	3.5	3.4	0.1
	15	3.1	3.0	0.1
	20	3.3	3.2	0.1
FCA+TPPO	10	3.8	3.7	0.1
	15	3.6	3.5	0.1
	20	4.3	4.2	0.1

Figure 31: Images of epoxy films incorporated with benzoic acid before and after the combustion.

Figure 32: Images of epoxy films incorporated with FCA before and after the combustion.

Figure 33: Images of epoxy films incorporated with FCA & TPPO before and after the combustion.

CHAPTER IV

CONCLUSION

Synthesis of FCA was accomplished in an 83% yield using a two-step process by reacting ferrocene with 2-chlorobenzoyl chloride followed by hydrolysis. FCA and BA were reacted with the epoxide using tetrabutylammonium bromide as a catalyst followed by thermal setting of the film with m-phenylene diamine. The epoxide films were characterized by FTIR and showed the expected absorbencies for the O-H, C-H. C=O and C-O.

Thermal properties of the epoxides were accessed using TGA, DSC, and a burn test. Epoxides with BA exhibited thermal stability of approximately 325^{o}C. Epoxides with FCA exhibited a slightly lower stability of approximately 305^{o}C. In addition, analyze of these graphs, show evident of which one is the best as flame retardant. Epoxide films showed corresponding Tg in the DSC test of 85, 100, and 105^{o}C for films with BA, FCA, and FCA+TPPO, respectively.

Burn test showed that epoxides with FCA had a significant reduction in flammability with burn time of 40 s or less and burn distances of approximately 0.1 in. These results showed the benefit of epoxides with FCA as a FR.

REFERENCES

1. Lu, S.-Y.; Hamerton, I., Recent developments in the chemistry of halogen-free flame retardant polymers. Progress in polymer science 2002, 27 (8), 1661-1712.
2. Hussein, M. A., & Asiri, A. M. (2012). Organometallic ferrocene-and phosphorus-containing polymers: synthesis and characterization. *Designed Monomers and Polymers*, *15*(3), 207-251.
3. Astruc, D. (2017). Why is ferrocene so exceptional?. *European Journal of Inorganic Chemistry*, *2017*(1), 6-29.
4. Shaw, S., Halogenated flame retardants: do the fire safety benefits justify the risks? *Reviews on environmental health* **2010,** *25* (4), 261-306.
5. Morgan, A. B.; Wilkie, C. A., The non-halogenated flame retardant handbook. John Wiley & Sons: 2014.
6. Mariappan, T.; Wilkie, C. A., Flame retardant epoxy resin for electrical and electronic applications. Fire and Materials 2014, 38 (5), 588-598.
7. Wade, L. G. Epoxide. https://www.britannica.com/science/epoxide (accessed 12th February).
8. Cripps, D. Epoxy Resins. https://netcomposites.com/guide-tools/guide/resin-systems/epoxy-resins/.
9. Rakotomalala, M.; Wagner, S.; Döring, M., Recent developments in halogen free flame retardants for epoxy resins for electrical and electronic applications. *Materials* **2010,** *3* (8), 4300-4327.

10. Liu, Y. L.; Hsiue, G. H.; Lee, R. H.; Chiu, Y. S., Phosphorus-containing epoxy for flame retardant. III: Using phosphorylated diamines as curing agents. Journal of Applied Polymer Science 1997, 63 (7), 895-901.
11. Mercado, L.; Galia, M.; Reina, J., Silicon-containing flame retardant epoxy resins: synthesis, characterization and properties. Polymer degradation and stability 2006, 91 (11), 2588-2594.
12. Hsiue, G. H.; Liu, Y. L.; Tsiao, J., Phosphorus-containing epoxy resins for flame retardancy V: Synergistic effect of phosphorus–silicon on flame retardancy. Journal of Applied Polymer Science 2000, 78 (1), 1-7.
13. Yang, S.; Zhang, Q.; Hu, Y., Synthesis of a novel flame retardant containing phosphorus, nitrogen and boron and its application in flame-retardant epoxy resin. Polymer Degradation and Stability 2016, 133, 358-366.
14. Astruc, D., History of Organometallic Chemistry. Organometallic Chemistry and Catalysis 2007, 5-20.
15. Werner, H., At least 60 years of ferrocene: the discovery and rediscovery of the sandwich complexes. Angewandte Chemie International Edition 2012, 51 (25), 6052-6058.
16. Liao, D.-J.; Xu, Q.-K.; McCabe, R. W.; Babu, H. V.; Hu, X.-P.; Pan, N.; Wang, D.-Y.; Hull, T. R., Ferrocene-Based Nonphosphorus Copolymer: Synthesis, High-Charring Mechanism, and Its Application in Fire Retardant Epoxy Resin. Industrial & Engineering Chemistry Research 2017, 56 (44), 12630-12643.

17. Daum, P.; Murray, R. W., Charge-transfer diffusion rates and activity relationships during oxidation and reduction of plasma-polymerized vinylferrocene films. The Journal of Physical Chemistry 1981, 85 (4), 389-396.
18. Zhu, Y.; Wolf, M. O., Charge transfer and delocalization in conjugated (ferrocenylethynyl) oligothiophene complexes. Journal of the American Chemical Society 2000, 122 (41), 10121-10125.
19. Carberry, J.; Irvin, J. A.; Glatzhofer, D. T.; Nicholas, K. M.; Neef, C. J., High molecular weight copolymers of vinylferrocene and 3-phenyl [5] ferrocenophane-1, 5-dimethylene with various N-substituted maleimides. Reactive and Functional Polymers 2013, 73 (5), 730-736.
20. Mehdipour-Ataei, S.; Babanzadeh, S., New types of heat-resistant, flame-retardant ferrocene-based polyamides with improved solubility. Reactive and Functional Polymers 2007, 67 (10), 883-892.
21. Zhou, W.; Wang, L.; Yu, H.; Yang, X.; Chen, Q.; Wang, J., Synthesis of a novel ferrocene-based epoxy compound and its burning rate catalytic property. RSC Advances 2016, 6 (59), 53679-53687.
22. Yu, H.; Wang, L.; Huo, J.; Tan, Q.; Gao, J., Synthesis of a novel ferrocene-based epoxy compound and its electrochemical behavior. Designed Monomers and Polymers 2008, 11 (4), 347-356.
23. Li, A., Xu, W., Wang, G., & Wang, X. (2018). Novel strategy for molybdenum disulfide nanosheets grown on titanate nanotubes for enhancing the flame retardancy and smoke suppression of epoxy resin. *Journal of Applied Polymer Science*, *135*(15).

24. Liu, L., Chen, X., & Jiao, C. (2015). Influence of ferrocene on smoke suppression properties and combustion behavior of intumescent flame-retardant epoxy composites. *Journal of Thermal Analysis and Calorimetry*, *122*(1), 437-447.
25. Giffin, Michael, "FERROCENE INCORPORATED INTO POLYURETHANES FOR IMPROVED FLAME-RETARDANT PROPERTIES" (2016).
26. Zhang, L., Wang, Y., & Cai, X. (2016). Effect of a novel polysiloxane-containing nitrogen on the thermal stability and flame retardancy of epoxy resins. *Journal of Thermal Analysis and Calorimetry*, *124*(2), 791-798.
27. Chen, P. F., Yan, K. K., Leng, J. X., Zhang, F., & Jiao, L. (2018). Synergistic smoke suppression effect of epoxy cross-linked structure and ferrocene on epoxy-based intumescent flame-retardant coating. *Plastics, Rubber and Composites*, 1-8.
28. Rozhnova, R.; Rudenchik, T.; Davidenko, V.; Bondarenko, P.; Galatenko, N., Effect of ferrocene on the structures and properties of epoxy-polyurethane composites. Polymer Science Series A 2014, 56 (3), 311-317.
29. Jones, B. H.; Wheeler, D. R.; Black, H. T.; Stavig, M. E.; Sawyer, P. S.; Giron, N. H.; Celina, M. C.; Lambert, T. N.; Alam, T. M., Stress Relaxation in Epoxy Thermosets via a Ferrocene-Based Amine Curing Agent. Macromolecules 2017, 50 (13), 5014-5024.
30. Organic Syntheses, Coll. Vol. 6, p.625 (1988); Vol. 56, p.28 (1977).
31. http://sdbs.db.aist.go.jp/sdbs/cgi-bin/cre_index.cgi
32. Gandara, I.S.; Mahia, P.L.; Losada, P.P.; Lozano, J.S; Abuin, S.P, Overall migration and specific migration of bisphenol A diglycidyl ether monomer and m-xylylenediamine hardener from an optimized epoxy-amine formulation into

water-based food simulants. Food Additives & contaminants 1993, 10(5), 555-565.

APPENDIX

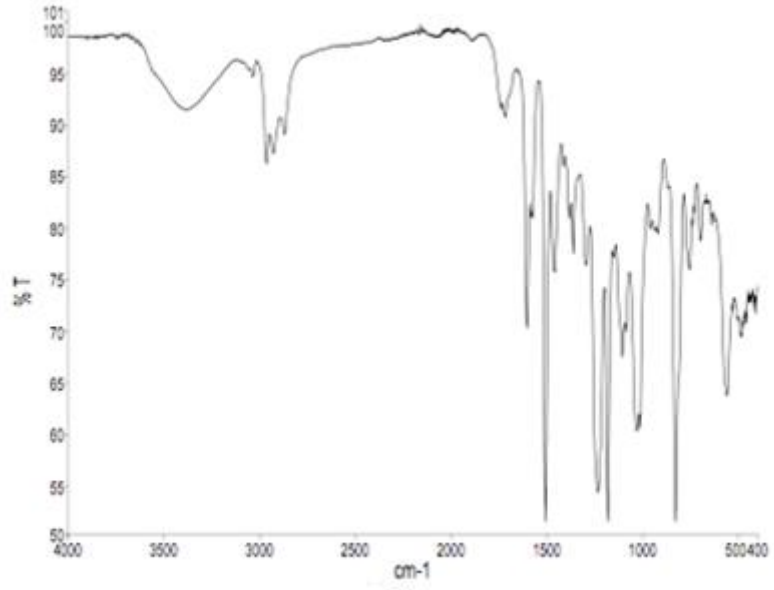

Figure 34: FT-IR spectrum of Epoxy Films incorporated with 15% benzoic acid.

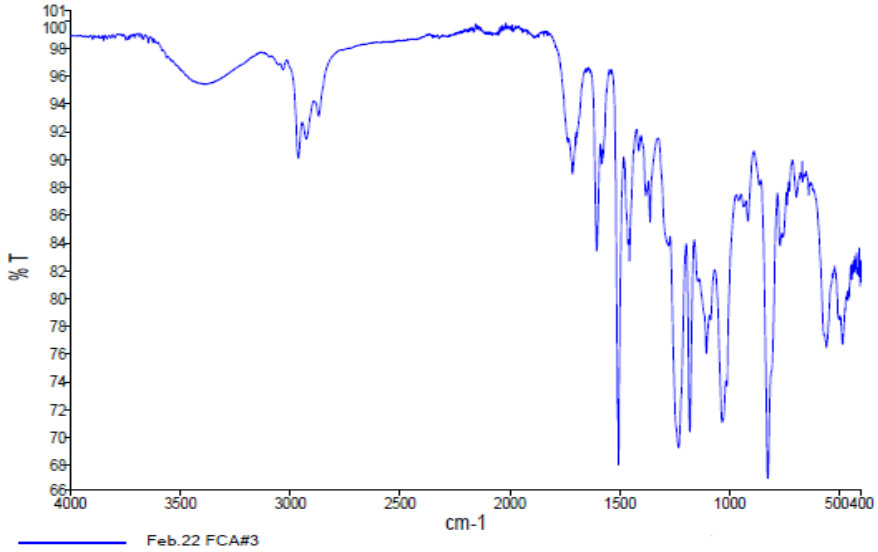

Figure 35: FT-IR spectrum of epoxy films incorporated with 15% FCA.

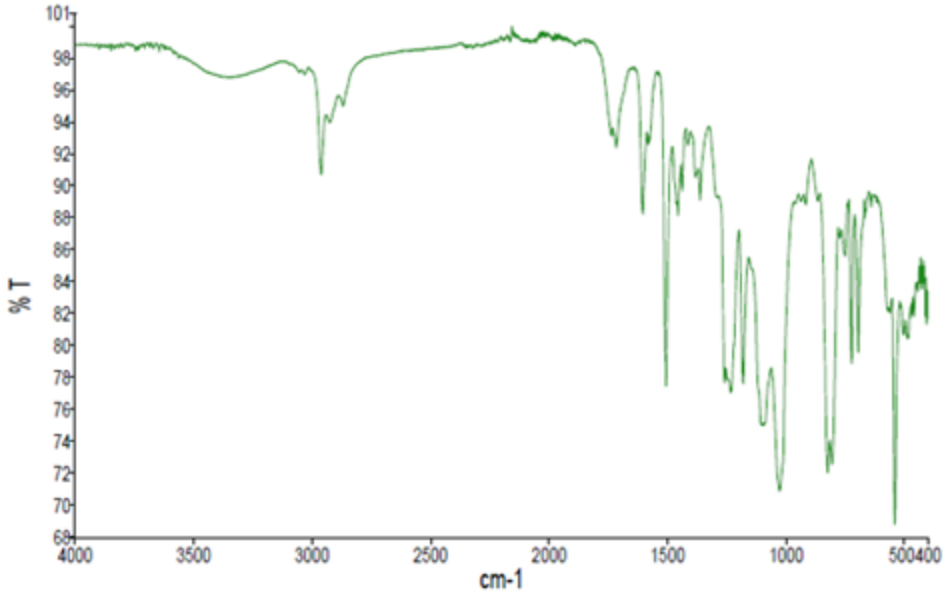

Figure 36: FT-IR of epoxy thin films incorporated with 15% of FCA & TPPO.

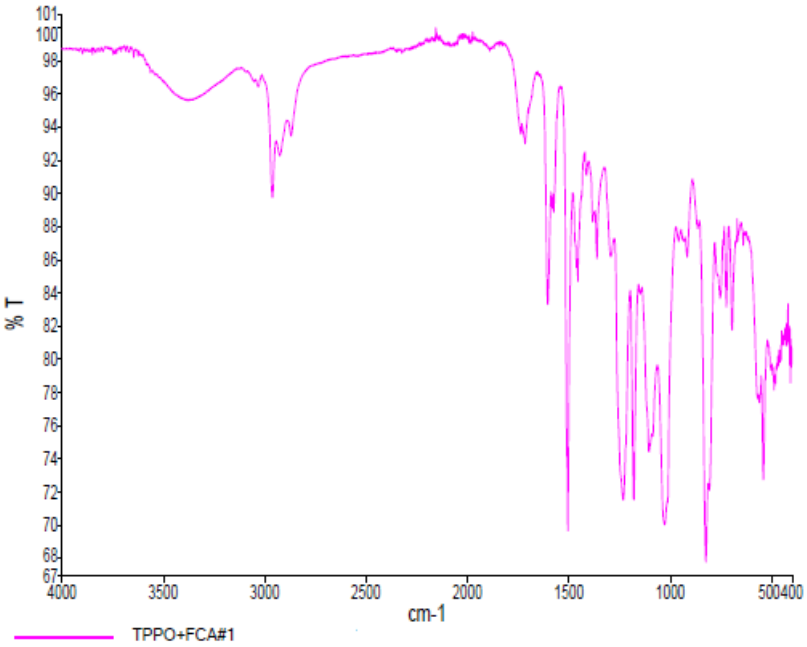

Figure 37: FT-IR of epoxy thin films incorporated with 20% of FCA & TPPO.